Research article

JHEP|Reports

Zinc finger transcription factor Egf1 promotes non-alcoholic fatty liver disease

Yan Guo,[1,†] **Xiulian Miao**,[1,†] **Xinyue Sun**,[2,†] Luyang Li,[3] Anqi Zhou,[1] Xi Zhu,[4] Yong Xu,[1,2] Qinghua Wang,[5,*] Zilong Li,[2,*] Zhiwen Fan[6,*]

[1]*Institute of Biomedical Research and College of Life Sciences, Liaocheng University, Liaocheng, China;* [2]*State Key Laboratory of Natural Medicines, Department of Pharmacology, China Pharmaceutical University, Nanjing, China;* [3]*Department of Oral Medicine, Affiliated Jiangning Hospital of Nanjing Medical University, Nanjing, China;* [4]*Department of Infectious Diseases, Kunshan First People's Hospital Affiliated to Jiangsu University, Kunshan, China;* [5]*Department of Gastroenterology, Kunshan First People's Hospital Affiliated to Jiangsu University, Kunshan, China;* [6]*Department of Pathology, Affiliated Nanjing Drum Tower Hospital, Nanjing University School of Medicine, Nanjing, China*

JHEP Reports **2023.** https://doi.org/10.1016/j.jhepr.2023.100724

Background & Aims: Non-alcoholic fatty liver disease (NAFLD) contributes to the global epidemic of metabolic syndrome and is considered a prelude to end-stage liver diseases such as cirrhosis and hepatocellular carcinoma. During NAFLD pathogenesis, hepatic parenchymal cells (hepatocytes) undergo both morphological and functional changes owing to a rewired transcriptome. The underlying mechanism is not entirely clear. In the present study, we investigated the involvement of early growth response 1 (Egr1) in NAFLD.

Methods: Quantitative PCR, Western blotting, and histochemical staining were used to assess gene expression levels. Chromatin immunoprecipitation was used to evaluate protein binding to DNA. NAFLD was evaluated in leptin receptor-deficient (*db*/*db*) mice.

Results: We report here that Egr1 was upregulated by pro-NAFLD stimuli *in vitro* and *in vivo*. Further analysis revealed that serum response factor (SRF) was recruited to the Egr1 promoter and mediated Egr1 transactivation. Importantly, Egr1 depletion markedly mitigated NAFLD in *db*/*db* mice. RNA sequencing revealed that Egr1 knockdown in hepatocytes, on the one hand, boosted fatty acid oxidation (FAO) and, on the other hand, suppressed the synthesis of chemoattractants. Mechanistically, Egr1 interacted with peroxisome proliferator-activated receptor α (PPARα) to repress PPARα-dependent transcription of FAO genes by recruiting its co-repressor NGFI-A binding protein 1 (Nab1), which potentially led to promoter deacetylation of FAO genes.

Conclusions: Our data identify Egr1 as a novel modulator of NAFLD and a potential target for NAFLD intervention.

Impact and Implications: Non-alcoholic fatty liver disease (NAFLD) precedes cirrhosis and hepatocellular carcinoma. In this paper, we describe a novel mechanism whereby early growth response 1 (Egr1), a transcription factor, contributes to NAFLD pathogenesis by regulating fatty acid oxidation. Our data provide novel insights and translational potential for NAFLD intervention.

Introduction

Non-alcoholic fatty liver disease (NAFLD) is a prototypic form of metabolic syndrome that affects 25% of the global population.[1] Without effective intervention, some patients with NAFLD will develop cirrhosis, hepatocellular carcinoma, and eventually liver failure. NAFLD shares many common pathological features with alcoholic liver disease (ALD), which include accumulation of lipid droplets, presence of extensive immune infiltrates, and hepatocyte ballooning.[2] Indeed, diagnostic criteria for NAFLD are similar to those for ALD except for long-term excessive alcohol consumption. In the past decade, NAFLD has become the primary contributor not only to end-stage liver diseases (*e.g.* cirrhosis) but also to cardiovascular diseases and diabetes.[3] Despite decades of rigorous research, therapeutic strategies for NAFLD remain elusive.[4]

Transcriptional reprogramming is considered key to the pathologies associated with NAFLD. For instance, increased expression levels of fatty acid transporters, which include members of the fatty acid transport proteins (FATP) family and CD36, are observed in the livers of patients with NAFLD compared with the healthy individuals.[5] Rate-limiting enzymes involved in *de novo* lipogenesis, including fatty acid synthase and acetyl-CoA carboxylase, are found to be upregulated during

Keywords: Non-alcoholic fatty liver disease; Transcriptional regulation; Transcription factor; Hepatocyte.

Received 8 November 2022; received in revised form 19 January 2023; accepted 22 February 2023; available online 9 March 2023

† These authors contributed to this work equally.

* Corresponding authors. Addresses: Kunshan First People's Hospital, Kunshan, China (Q. Wang); China Pharmaceutical University, Nanjing, China (Z. Li); Nanjing Drum Tower Hospital, Nanjing, China (Z. Fan).

E-mail addresses: 20214132092@stu.suda.edu.cn (Q. Wang), lzl1114@cpu.edu.cn (Z. Li), fanzhiwenfff@126.com (Z. Fan).

NAFLD pathogenesis in humans and in experimental animals,[6,7] likely owing to elevated activity of sterol response element binding protein (SREBP). On the contrary, genes that encode enzymes participating in fatty acid oxidation (FAO) appear to be lower in patients with NAFLD than in healthy individuals, which can be attributed to deficiencies of the transcription factor peroxisome proliferator-activated receptor α (PPARα).[8,9] Thus, enhanced lipid uptake and synthesis in combination with suppressed FAO may help explain hepatic lipid accumulation associated with NAFLD. Upregulation of TRAF3, a key adaptor molecule in the tumour necrosis factor signalling pathway, in hepatocytes by free fatty acids (FAA) as a result of excessive energy influx has been reported.[10] Consequently, NF-κB, the master regulator of pro-inflammatory transcription, is activated to program the synthesis of pro-inflammatory mediators.[11] Of note, many of the transcription factors are considered 'versatile' in coordinating pro-NAFLD transcriptional events. For instance, SREBP1c has been documented to modulate the transcription of pro-inflammatory mediators.[12–14] On the contrary, there is also evidence to implicate NF-κB in lipid metabolism: NF-κB unorthodoxly represses the transcription of Sorcin, which in turn promotes carbohydrate response element binding protein (ChREBP) nuclear accumulation to influence *de novo* lipogenesis.[15] Recently, it has been demonstrated that multiple networks of transcription factors contribute to the overhaul of hepatic transcriptome during NAFLD pathogenesis.[16]

Early growth response 1 (Egr1) was independently isolated and characterised by the Siebenlist laboratory[17] and the Forsdyke laboratory[18] as an early inducible gene in the process of T lymphocyte expansion. Egr1 is a zinc finger transcription factor that plays roles in a wide range of pathophysiological processes including host defence response, carcinogenesis, and organ fibrosis.[19–21] Previously, Nagi and colleagues have shown that Egr1 expression was upregulated in the livers of rodents fed an ethanol diet to induce ALD.[22] Moreover, Egr1 deletion completely abrogated alcohol-induced liver injury in mice likely owing to dampened hepatic inflammation.[22] Because of the overall similarity between NAFLD and ALD pathogenesis, we hypothesised that Egr1 might contribute to NAFLD development by regulating transcription in hepatocytes exposed to FAA. We report here that Egr1 expression is regulated by pro-NAFLD stimuli, likely mediated by serum response factor (SRF), in hepatocytes *in vivo* and *in vitro*. Importantly, Egr1 regulates transcriptional events relevant to the pathogenesis of NAFLD. Therefore, our data identify Egr1 as a novel modulator of NAFLD and a potential target for NAFLD intervention.

Materials and methods

Animals

All the animal experiments were reviewed and approved by the Liaocheng University Ethics Committee on Humane Treatment of Experimental Animals. The mice were maintained in an SPF environment with 12-h light/dark cycles and libitum access to food and water. NAFLD was induced by four different protocols: (1) *db*/*db* mice on a regular chow diet for 12 wk; (2) C57/B6 mice on a high-fat diet (HFD; D09100310, Research Diets) for 12 wk; (3) *Apoe*$^{-/-}$ mice on a Western diet (D12079B, Research Diets, New Brunswick, NJ, USA) for 7 wk; and (4) C57/B6 mice on choline-deficient, L-amino acid-defined HFD (CDA-HFD; A06071309, Research Diets) for 8 wk as previously described.[23] In certain experiments, Egr1-targeting small-hairpin RNA (shRNA) was placed downstream of the human thyroxin-binding globulin (TBG) promoter and packed into AAV8 for tail vein injection into *db*/*db* mice.

Cell culture, plasmids, and transient transfection

Human hepatoma cells (HepaRG, Thermo Fisher, San Jose, CA, USA) were maintained in DMEM supplemented with 10% FBS (Hyclone, Logan, UT, USA). Primary murine hepatocytes were isolated as previously described[24,25] and seeded at 2 × 10^5 cells/well for 12-well culture dishes, or 4 × 10^5 cells/well for 6-well culture dishes, or 4 × 10^6 cells/well for p100 culture dishes. Cell viability was examined at the time of seeding by trypan blue staining; typical isolation yielded >95% viability. *EGR1* promoter-luciferase construct was generated by amplifying genomic DNA spanning the proximal promoter and the first exon of EGR1 gene (-900/+50) and ligating into a pGL3-basic vector (Promega, Madison, WI, USA). Truncation mutants were made using a QuikChange kit (Thermo Fisher Scientific, Waltham, MA, USA) and verified by direct sequencing. Small interfering RNAs (siRNAs) were purchased from Dharmacon (Lafayette, CO, USA). Transient transfections were performed with Lipofectamine 2000 (Thermo Fisher Scientific). Luciferase activities were assayed 24–48 h after transfection using a luciferase reporter assay system (Promega) as previously described.[26]

RNA isolation and real-time PCR

RNA was extracted with the RNeasy RNA isolation kit (Qiagen, Germantown, MD, USA) as previously described.[27,28] Reverse transcriptase reactions were performed using a SuperScript First-strand Synthesis System (Invitrogen, Waltham, MA, USA). Real-time PCRs were performed on an ABI Prism 7500 system using the following primers: mouse *Egr1*, TCGGCTCCTTTCCTCACTCA and CTCATAGGGTTGTTCGCTCGG; human *EGR1*, GGTCAGTGGCCTAGTGAGC and GTGCCGCTGAGTAAATGGGA; mouse *Il1b*, GAAATGCCACCTTTTGACAGTG and TGGATGCTCTCATCAGGACAG; mouse *Il6*, TGGGGCTCTTCAAAAGCTCC and AGGAACTATCACCGGATCTTCAA; mouse *Mcp1*, AAAACACGGGACGAGAAACCC and ACGGGAACCTTTATTAACCCCT; and mouse *Tnfa*, CTGGATGTCAATCAACAATGGGA and ACTAGGGTGTGAGTGTTTTCTGT. Ct values of target genes were normalised to the Ct values of the housekeeping control gene (18s, 5′-CGCGGTTCTATTTTGTTGGT-3′ and 5′-TCGTCTTCGAAACTCCGACT-3′ for both human and mouse genes) using the ΔΔCt method and expressed as relative mRNA expression levels compared with the control group, which is arbitrarily set as 1.

Protein extraction and Western blot

Whole-cell lysates were obtained by resuspending cell pellets in radioimmunoprecipitation assay (RIPA) buffer (50 mM Tris pH7.4, 150 mM NaCl, 1% Triton X-100) with freshly added protease inhibitor (Roche, Basel, Switzerland) as previously described.[29] Typically, 100 μl RIPA buffer was used for 1 × 10^6 cells. Moreover, 30 μg of protein was loaded in each lane and separated by 8% SDS-PAGE gel with all-blue protein markers (Bio-Rad, Hercules, CA, USA). Proteins were transferred to nitrocellulose membranes (Bio-Rad) in a Mini-Trans-Blot Cell (Bio-Rad). The membranes were blocked with 5% fat-free milk powder in TBS at room temperature for half an hour and then incubated with the following primary antibodies at 4 °C overnight: anti-Egr1 (Proteintech, Wuhan, China, 55117-1, 1:500) and anti-β-actin (Sigma, Burlington, MA, USA, A1978, 1:5,000). The next day, the membranes were washed with TBS and incubated

with horseradish peroxidase (HRP)-conjugated anti-rabbit secondary antibody (Thermo Fisher, 61-6520, 1:5,000) or anti-mouse secondary antibody (Thermo Fisher, 31464, 1:5,000) for 1 h at room temperature. For densitometrical quantification, densities of target proteins were normalised to those of β-actin. Data are expressed as relative protein levels compared with the control group, which is arbitrarily set as 1.

Chromatin immunoprecipitation

Chromatin immunoprecipitation (ChIP) assays were performed essentially as described before.[30,31] Chromatin was cross-linked with 1% formaldehyde for 8 min at room temperature and then sequentially washed with ice-cold PBS, solution I (10 mM HEPES, pH 7.5, 10 mM EDTA, 0.5 mM EGTA, 0.75% Triton X-100), and solution II (10 mM HEPES, pH 7.5, 200 mM NaCl, 1 mM EDTA, 0.5 mM EGTA). Cells were incubated in lysis buffer (150 mM NaCl, 25 mM Tris pH 7.5, 1% Triton X-100, 0.1% SDS, 0.5% deoxycholate) supplemented with protease inhibitor tablet. DNA was fragmented into 500-bp pieces using a Branson 250 sonicator (Brookfield, CT, USA). Aliquots of lysates containing 100 μg of protein were used for each immunoprecipitation reaction with anti-SRF (Cell Signaling Tech, Danvers, MA, USA, 5147), anti-Egr1 (Cell Signaling Tech, 4154), anti-NGFI-A binding protein 1 (Nab1) (Novus Biologicals, Minneapolis, MN, USA, NBP1-71838), anti-acetyl H3K9 (Millipore, Burlington, MA, USA, 07-352), anti-acetyl H3K27 (Millipore, Burlington, MA, USA 07-360), anti-acetyl H3K14 (Millipore, Burlington, MA, USA, 07-353), anti-acetyl H3K18 (Millipore, 07-354), or IgG followed by adsorption to protein A/G PLUS-agarose beads (Santa Cruz Biotechnology, Santa Cruz, CA, USA). Precipitated DNA–protein complexes were washed sequentially with RIPA buffer (50 mM Tris, pH 8.0, 150 mM NaCl, 0.1% SDS, 0.5% deoxycholate, 1% Nonidet P-40, 1 mM EDTA), high salt buffer (50 mM Tris, pH 8.0, 500 mM NaCl, 0.1% SDS, 0.5% deoxycholate, 1% Nonidet P-40, 1 mM EDTA), LiCl buffer (50 mM Tris, pH 8.0, 250 mM LiCl, 0.1% SDS, 0.5% deoxycholate, 1% Nonidet P-40, 1 mM EDTA), and TE buffer (10 mM Tris,1 mM EDTA, pH 8.0). DNA–protein cross-link was reversed by heating the samples to 65 °C overnight. Proteins were digested with proteinase K (Sigma), and DNA was phenol/chloroform-extracted and precipitated by 100% ethanol. Precipitated genomic DNA was amplified by real-time PCR.

Human NASH biopsy specimens

Liver biopsies were collected from patients with non-alcoholic steatohepatitis (NASH) referring to the First People's Hospital of Changzhou. Control liver samples were collected from donors without NASH but deemed unsuitable for transplantation. Written informed consent was obtained from participants or families of liver donors. All procedures that involved human samples were approved by the Ethics Committee of the First People's Hospital of Changzhou and adhered to the principles outlined in the Declaration of Helsinki.

Glucose tolerance assays

For the glucose tolerance test (GTT), mice fasted overnight were injected i.p. with 2 g/kg glucose, and blood samples were taken at the indicated intervals. For the insulin tolerance test (ITT), mice were fasted for 6 h and injected i.p. with 0.75 IU/kg soluble insulin, and blood samples were taken at the indicated intervals. For the pyruvate tolerance test, mice were fasted for 6 h and injected i.p. with 2.5 g/kg pyruvate dissolved in PBS, and blood samples were taken at the indicated intervals. Blood glucose was measured using an Accu-Chek compact glucometer (Roche).

Histology

Histological analyses were performed essentially as described before.[32] Images were taken using an Olympus IX-70 microscope (Shinjuku, Tokyo, Japan). Quantifications were performed with ImageJ. For each mouse, at least three slides were stained, and at least five different fields were analysed for each slide.

RNA sequencing and data analysis

RNA sequencing (RNA-seq) was performed as previously described.[33] Total RNA was extracted using the TRIzol reagent (Thermo Fisher Scientific) according to the manufacturer's protocol. RNA purity and quantification were evaluated using the NanoDrop 2000 spectrophotometer (Thermo Scientific). RNA integrity was assessed using the Agilent 2100 Bioanalyzer (Agilent Technologies, Santa Clara, CA, USA). Then, the libraries were constructed using the TruSeq Stranded mRNA LT Sample Prep Kit (Illumina, San Diego, CA, USA) according to the manufacturer's instructions and sequenced on an Illumina HiSeq X Ten platform, and 150-bp paired-end reads were generated. Raw data (raw reads) of fastq format were firstly processed using Trimmomatic, and the low-quality reads were removed to obtain the clean reads. The clean reads were mapped to the mouse genome (Mus_musculus.GRCm38.99) using HISAT2. FPKM (fragments per kilobase of exon model per million reads mapped) of each gene was calculated using Cufflinks, and the read counts of each gene were obtained using HTSeqcount. Differential expression analysis was performed using the DESeq (2012) R package. A p value <0.05 and fold change >2 or fold change <0.5 were set as the thresholds for significantly differential expression. Hierarchical cluster analysis of differentially expressed genes (DEGs) was performed to demonstrate the expression pattern of genes in different groups and samples. Gene ontology (GO) enrichment and Kyoto Encyclopedia of Genes and Genomes (KEGG) pathway enrichment analysis of DEGs were performed respectively using R based on the hypergeometric distribution.

Statistical analysis

For comparison between two groups, a two-tailed t test was performed. For comparison among three or more groups, one-way ANOVA or two-way ANOVA with *post hoc* Turkey analyses were performed using an SPSS package (IBM Corp., Armonk, NY, USA). The assumptions of normality were checked using the Shapiro–Wilk test, and equal variance was checked using Levene's test; both were satisfied. Values of p less than 0.05 were considered statistically significant (*). All *in vitro* experiments were repeated at least three times, and three replicates were estimated to provide 80% power.

Results

Egr1 expression is upregulated by pro-NAFLD stimuli *in vitro* and *in vivo*

The following experiments were performed to determine whether Egr1 expression was altered during NAFLD pathogenesis in four different animal models. In the livers of 12-wk db/*db* mice, Egr1 expression at both mRNA levels (Fig. 1A) and protein levels (Fig. 1B) was appreciably higher than that in the livers of *db*/+ mice. In the second model, male C57/B6 mice were fed an HFD for 12 wk. Compared with the mice fed

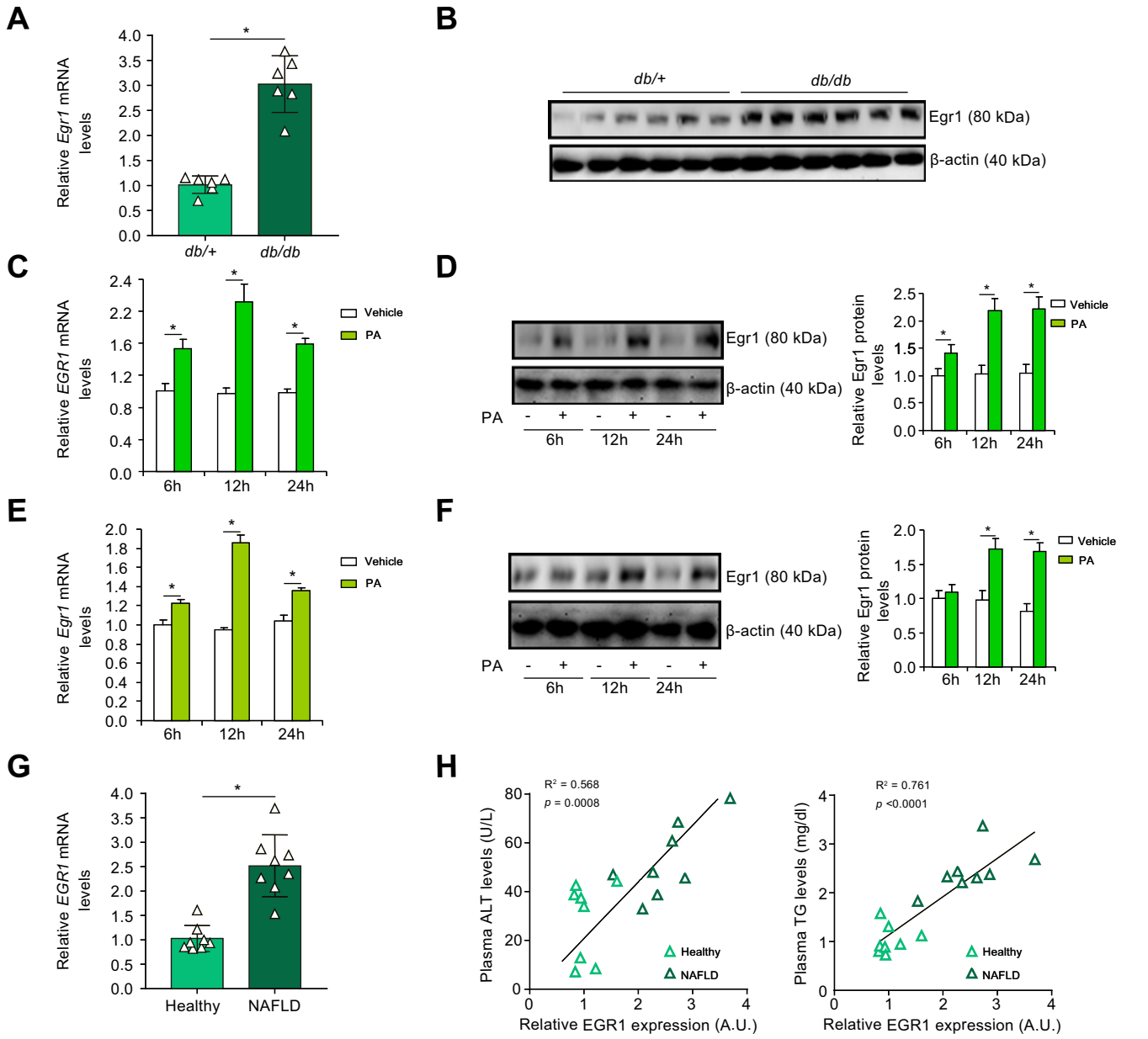

Fig. 1. Egr1 is upregulated by pro-NAFLD stimuli *in vivo* and *in vitro*. (A and B) Egr1 expression in the liver tissues of 12-wk male *db*/*db* mice and *db*/+ mice was examined by qPCR and Western blotting. N = 6 mice for each group. Data are expressed as mean ± SD. **p* <0.05, two-tailed Student's *t* test. (C and D) HepaRG cells were treated with or without PA (0.2 mM). EGR1 expression was examined by qPCR and Western blotting. N = 3 biological replicates. Data are expressed as mean ± SD. **p* <0.05, two-tailed Student's *t* test. (E and F) Primary hepatocytes were treated with or without PA (0.2 mM). Egr1 expression was examined by qPCR and Western blotting. N = 3 biological replicates. Data are expressed as mean ± SD. **p* <0.05, two-tailed Student's *t* test. (G and H) Egr1 expression levels in the livers of patients with NASH and healthy individuals were examined by qPCR. Linear regression was performed by GraphPad Prism (Dotmatics, Boston, MA, USA). N = 8 cases for each group. Data are expressed as mean ± SD. **p* <0.05. ALT, alanine transaminase; Egr1, early growth response 1; NAFLD, non-alcoholic fatty liver disease; NASH, non-alcoholic steatohepatitis; PA, palmitate; qPCR, quantitative PCR; TG, triglyceride.

with the control diet (CD), Egr1 expression was significantly upregulated in the livers of the mice fed the HFD (Fig. S1). In the third model, male *Apoe*$^{-/-}$ mice were fed a Western diet for 7 wk. Higher expression levels of Egr1 were detected in the livers of mice fed the Western diet than in those fed the CD (Fig. S2). In the fourth model, male C57/B6 mice were fed a CDA-HFD for 8 wk. Again, more Egr1 molecules were detected in the CDA-HFD-fed livers than in the CD-fed livers (Fig. S3).

FFA, including palmitate (PA), are among the best characterised risk factors for NAFLD.[34] When primary murine hepatocytes were exposed to PA, a small but significant upregulation of Egr1 expression was detected as early as 6 h after the treatment (Fig. 1C and D). Egr1 expression peaked at 12 h and declined at 24 h. Similar observations were made in the human hepatoma cells (HepaRG): the cells responded to PA treatment by upregulating Egr1 expression fast and transiently (Fig. 1E and F). However, Egr1 expression was unaltered in cells exposed to

oleate (Fig. S4), pointing to certain level of selectivity in terms of the responsiveness of Egr1 to nutrients/metabolites. In addition, Egr1 expression could be stimulated in hepatocytes exposed to fructose (Fig. S5), another major risk factor for NAFLD.[35]

Liver specimens collected from patients with NAFLD and healthy donors were examined for Egr1 expression. As shown in Fig. 1G, Egr1 levels were markedly elevated in individuals diagnosed with NAFLD compared with those in healthy individuals. More importantly, a positive correlation was identified between Egr1 expression and steatotic injuries (as measured by plasma alanine transaminase [ALT] and triglyceride levels) in humans (Fig. 1H). Together, these data support the conclusion that Egr1 expression may be associated with NAFLD pathogenesis.

SRF mediates Egr1 transactivation in hepatocytes

To determine whether the observed upregulation of Egr1 expression occurred at the transcriptional level, an Egr1 promoter-luciferase construct (-900/+50) was transfected into HepaRG cells; PA treatment led to a robust augmentation of the Egr1 promoter activity (Fig. 2A). A host of transcription factors have been identified to bind to the Egr1 promoter and regulate Egr1 gene transcription, which include E26 transformation-specific (ETS), cAMP response element binding protein (CREB), activator protein 1 (AP-1), SRF, and NF-κB (Fig. 2A). Progressive deletions introduced to the Egr1 promoter did not alter its responsiveness to PA treatment unless a string of SRF binding sites located between -400 and -200 relative to the transcription start site (TSS) was removed (Fig. 2A). Of note, PA treatment did not significantly alter SRF expression at either mRNA levels (Fig. S6A) or protein levels (Fig. S6B). Immunofluorescence staining showed that PA treatment altered SRF subcellular localisation in hepatocytes: in the absence of PA, SRF was detected in both the cytoplasm and the nucleus; in the presence of PA, SRF was almost exclusively detected in the nucleus (Fig. S6C). ChIP assay confirmed that PA treatment resulted in enhanced binding of SRF to the Egr1 promoter consistent with its nuclear accumulation (Fig. 2B). Enhanced binding of SRF to the Egr1 promoter was also detected in the livers of the *db*/*db* mice compared with the *db*/+ mice (Fig. S7). Compared with the wild-type Egr1 promoter-luciferase construct, a mutant construct without the SRF motif completely lost the response to PA treatment (Fig. 2C). Finally, knockdown of SRF expression by two different pairs of siRNAs attenuated Egr1 induction by PA treatment in hepatocytes (Fig. 2D–G). Of note, SRF knockdown appeared to significantly dampen Egr1 induction by fructose in both HepaRG cells and murine primary hepatocytes (Fig. S8). Collectively, these data support the conclusion that SRF mediates Egr1 transactivation in hepatocytes.

Egr1 depletion attenuates NAFLD in mice

Next, lentivirus carrying shRNA targeting Egr1 (shEgr1) (Lenti-shEgr1) or a control shRNA (shC) (Lenti-shC) was injected into *db*/*db* mice to determine whether Egr1 interference would alter NAFLD *in vivo* (Fig. 3A); quantitative PCR (qPCR) and Western blotting confirmed that Egr1 levels were downregulated by Lenti-shEgr1 injection compared with Lenti-shC injection (Fig. S9). Egr1 silencing did not impact the body weight of the mice (Fig. S10). Nor did Egr1 silencing influence JNK signalling in the liver (Fig. S11). However, insulin sensitivity, as measured by the glucose tolerance test (Fig. 3B) and the insulin tolerance test (Fig. 3C), was greatly improved by Egr1 knockdown. In addition, biochemical analysis of plasma ALT/aspartate aminotransferase (AST) levels (Fig. 3D and E), plasma triglyceride/cholesterol levels (Fig. 3F and G), and hepatic triglyceride/cholesterol levels (Fig. 3H and I) pointed to an amelioration of steatotic injury in the shEgr1-injected mice compared with the shC-injected mice. Histological staining showed that Egr1 knockdown reduced lipid accumulation, immune cell infiltration, deposition of extracellular matrix proteins, and reactive oxygen species (ROS) in the liver (Fig. 3J). Finally, expression levels of pro-inflammatory/fibrogenic mediators were collectively downregulated following Egr1 depletion in the *db*/*db* mice (Fig. 3K).

Egr1 knockdown alters transcriptome in hepatocytes

To gain genome-wide perspective on the role of Egr1 in NAFLD pathogenesis, RNA-seq analysis was performed to compare the transcriptome of hepatocytes before and after Egr1 was depleted with siRNAs. As shown in Fig. 4A, Egr1 knockdown significantly altered cellular transcriptome. Using 1.5 × fold change and $p < 0.05$ as thresholds, approximately 1,000 genes were identified to be altered by Egr1 knockdown (Fig. 4B). GO analysis (Fig. 4C) and KEGG analysis (Fig. 4D) indicated that Egr1 knockdown primarily influenced genes involved in cellular metabolism. Further, gene set enrichment analysis (GSEA) illustrated that Egr1 depletion was positively correlated with pathways involved in fatty acid metabolism but inversely correlated with pathways that promote hepatocyte-derived chemoattractive cues (Fig. 4E). Among the top DEGs were pro-inflammatory chemokines/cytokines (downregulated), antioxidants (upregulated), and fatty acid β-oxidation enzymes (upregulated) (Fig. 4F). In congruence, hypergeometric optimisation of motif enrichment (HOMER) analysis revealed that Egr1 deficiency attenuated the activities of pro-inflammatory transcription factors including NF-κB but liberated the activities of metabolic nuclear receptors including PPARα (Fig. 4G). Thus, it is possible that Egr1 might contribute to NAFLD by modulating lipid metabolism and inflammation in hepatocytes.

Erg1 interacts with PPARα to repress FAO transcription

Bioinformatic analysis offered compelling evidence for a potential interplay between Egr1 and PPARα. Co-immunoprecipitation assays showed that (1) ectopically expressed Egr1 and PPARα formed a complex in HEK293 cells (Fig. 5A) and (2) endogenous Egr1 and PPARα interacted with each other in the murine livers (Fig. 5B). Importantly, ChIP assay detected strong association of Egr1 with FAO gene promoters, all known PPARα targets, surrounding the PPAR response element (PPRE) in the *db*/*db* mice compared with the *db*/+ mice (Fig. 5C). Overexpression of Egr1 dose-dependently repressed PPARα activity measured by a reporter fused to six tandem repeats of PPRE (Fig. 5D). On the contrary, Egr1 knockdown significantly upregulated FAO genes in the *db*/*db* mice as measured by qPCR (Fig. 5E). Consistently, plasma ketone body (β-hydroxybutyrate) levels were higher in the shEgr1 mice than in the shC mice (Fig. S12). The hepatokine fibroblast growth factor 21 (FGF21) is a well-established PPARα target implicated in FAO.[36,37] However, FGF21 levels were not significantly altered by Egr1 knockdown in *db*/*db* mice or in primary hepatocytes (Fig. S13). Because FAO is a key physiological process during fasting, Egr1 expression was examined in the livers isolated from mice subjected to 12 h of fasting followed by 12 h of refeeding. Egr1 expression was mildly but significantly downregulated in the liver following fasting but returned to basal levels following refeeding (Fig. S14).

Previous studies indicate that Egr1 relies on co-repressor Nab1 to repress transcription.[38] Indeed, Nab1 was detected on

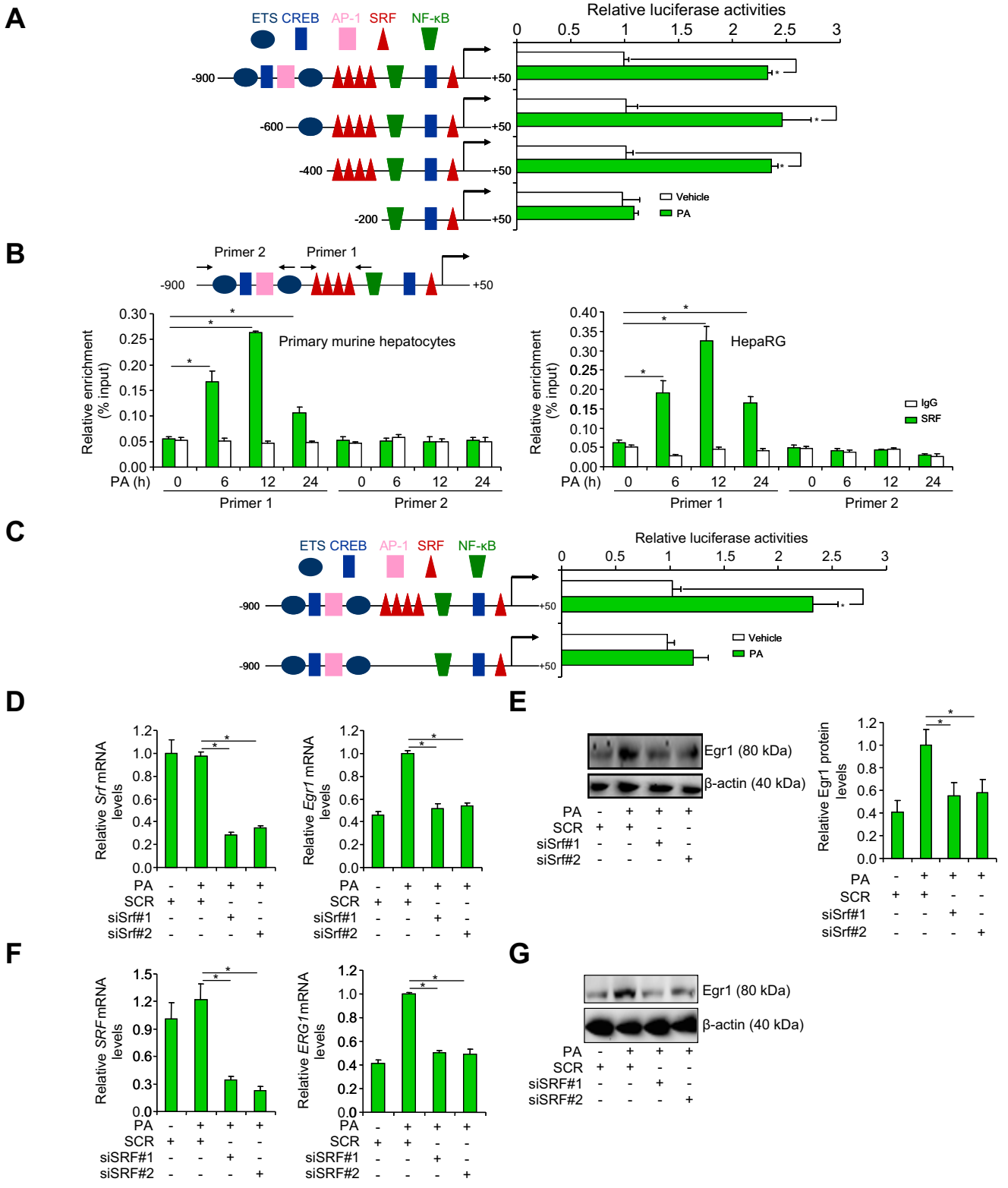

Fig. 2. SRF mediates Egr1 transactivation in hepatocytes. (A) Egr1 promoter-luciferase constructs were transfected into HepaRG cells followed by treatment with PA for 12 h. Luciferase activities were normalised by protein concentration and GFP fluorescence. N = 3 biological replicates. Data are expressed as mean ± SD. *p <0.05, two-tailed Student's t test. (B) Primary hepatocytes and HepaRG cells were treated with or without PA (0.2 mM). ChIP assay was performed with anti-SRF or IgG. N = 3 biological replicates. Data are expressed as mean ± SD. *p <0.05, one-way ANOVA with the *post hoc* Scheffé test. (C) Wild-type and mutant Egr1 promoter-luciferase constructs were transfected into HepaRG cells followed by treatment with PA for 12 h. Luciferase activities were normalised by protein concentration and GFP fluorescence. N = 3 biological replicates. Data are expressed as mean ± SD. *p <0.05, two-tailed Student's t test. (D and E) Primary hepatocytes were transfected with siRNA targeting SRF or SCR followed by treatment with PA (0.2 mM). Egr1 expression was examined by qPCR and Western blotting. N = 3 biological replicates. Data are expressed as mean ± SD. *p <0.05, one-way ANOVA with the *post hoc* Scheffé test. (F and G) HepaRG cells were

the FAO gene promoters, in a similar fashion as Egr1, in the *db*/*db* mice compared with the *db*/+ mice (Fig. 5F). Consistently, the Egr1 mutant that lacks the Nab1 interaction domain (Egr1Δ)[39] lost the ability to repress PPARα activity (Fig. 5G) and PPARα-dependent transactivation of FAO genes (Fig. 5H). In addition, Nab1 levels were found to be higher in the patients with NAFLD than in healthy individuals and correlated with steatotic injuries (Fig. S15).

Erg1 regulates FAO transcription by promoting histone deacetylation

Histone acetylation is considered a prototypical marker for actively transcribed chromatin. ChIP assay demonstrated that Egr1 deficiency significantly augmented acetylation of histone H3K9 (Fig. 6A), H3K14 (Fig. 6B), H3K18 (Fig. 6C), and H3K27 (Fig. 6D) on FAO gene promoters consistent with the upregulation of these genes. In HepaRG cells, exposure to the PPARα agonist evoked accumulation of acetylated histones on the FAO gene promoters, which was suppressed by wild-type Egr1 but not by Egr1Δ (Fig. 7A–D). These observations suggest that Erg1 might recruit histone deacetylases (HDACs), likely via Nab1, to the FAO promoters to repress transcription. To authenticate this hypothesis, two pan-HDAC inhibitors (HDACis), were exploited. As shown in Fig. 7E, repression of PPARα-induced FAO gene expression by Egr1 was partially relieved by co-treatment of either HDACi.

Discussion

Stimuli that promote NAFLD pathogenesis elicit profound changes in hepatocytes.[40] In the course of NAFLD development and progression, multiple transcription factors form extensive regulatory networks to influence transcriptome in hepatocytes.[41] We describe here a novel finding that Egr1, a transcription factor previously reported to regulate the pathogenesis of ALD, appears to be upregulated during NAFLD development in mice and in hepatocytes exposed to FFA. Moreover, single-gene and genome-wide profiling of expression patterns in hepatocytes indicate that Egr1 knockdown may dampen NAFLD pathogenesis. Thus, it is possible that Egr1 might represent a novel biomarker and a potential therapeutic target for NAFLD.

Our data indicate that SRF mediates PA-induced transactivation of Egr1 in hepatocytes by binding to the Egr1 promoter. Although SRF has been implicated in the regulation of multiple pathophysiological processes related to NAFLD, including inflammation,[42] production of ROS,[43] and lipid metabolism,[44] no direct evidence exists to link SRF to NAFLD pathogenesis, probably owing to a lack of suitable genetic tools. Sun *et al.*[45] have previously made an attempt to specifically delete SRF in hepatocytes by crossing the $Srf^{f/f}$ mice to the *Alb*-Cre mice. The resulting SRF conditional knockout mice were born at sub-Mendelian ratio, and the surviving mice displayed retarded growth compared with the wild-type littermates, which could be attributed to disruption of glucose and fat metabolism. These abnormalities, although preclude the analysis of NAFLD pathogenesis, suggest that SRF may be indispensable for the maintenance of physiological homoeostasis of the liver. Of interest, a study by Jin *et al.*[46] has found that nuclear accumulation of SRF in skeletal muscle cells exposed to PA correlated with a gene signature of insulin resistance. Our observation that PA treatment promoted migration of SRF into the nucleus in hepatocytes echoes that by Jin *et al.*[46] and suggests SRF might be a nutrition sensor that contributes to the regulation of insulin response.

A key finding of the present study is that Egr1 contributes to NAFLD pathogenesis by suppressing fatty acid β-oxidation in hepatocytes. Egr1 and its co-repressor repress FAO gene transcription by recruiting an HDAC activity. Concordantly, treatment with two pan-HDACis relieved the repression of FAO gene transcription. However, the identity of the specific HDAC(s) mediating repression of FAO gene transcription by Egr1 remains obscure. As such, whether HDACi administration could bring about any beneficial effects in established NAFLD models *in vivo* awaits to be tested. It should be noted that existing literature alludes to distinct roles for different HDACs in NAFLD pathogenesis. There is strong evidence to suggest that HDAC3, a class I HDAC, protects against NAFLD by promoting lipid metabolism, although this effect is likely deacetylase activity independent.[47] It has also been reported that HDAC5, a class IIa HDAC, promotes FAO and safeguards against liver steatosis in a PPARα-dependent manner.[48] On the contrary, both HDAC11,[49] the sole class IV HDAC, and HDAC1,[50] the ubiquitously expressed class I HDAC, appear to suppress FAO in the skeletal muscle and liver, respectively. Future studies should aim to unravel the precise epigenetic mechanism whereby Egr1 (re) programs cellular metabolism.

We show here that Egr1 knockdown in hepatocytes results in downregulation of several pro-inflammatory mediators. This is consistent with a previous report by Mackman and colleagues, in which it was found that the same set of pro-inflammatory mediators including IL-6 and monocyte chemoattractant protein 1 (MCP1) was repressed in the lungs and kidneys of Egr1 knockout mice compared with those of the wild-type mice in a model of lipopolysaccharide-induced endotoxaemia.[51] In addition, Cho *et al.*[52] have presented evidence to show that Egr1 deletion blunted pulmonary inflammation in IL-13 transgenic mice. Further, it has been documented that Egr1 deletion attenuates atherosclerotic lesions in $Ldlr^{-/-}$ mice fed a Western diet.[53] Because atherosclerosis is considered a prototypical pathology of chronic inflammation, it is tempting to speculate that Egr1 might be a master regulator of inflammatory response. However, a recent study by the Gardini laboratory indicated that Egr1 is able to bind to non-classic motifs located on the enhancers and repress the transcription of several pro-inflammatory genes in macrophages.[54] More studies are certainly warranted to reconcile this discrepancy.

Our RNA-seq data show that Egr1 knockdown is associated with upregulation of a panel of antioxidant genes, suggesting that Egr1 might contribute to NAFLD pathogenesis by altering redox homoeostasis. There has been abundant evidence that connects Egr1 expression/activity and intracellular ROS levels.

transfected with siRNA targeting SRF or SCR followed by treatment with PA (0.2 mM). Egr1 expression was examined by qPCR and Western blotting. N = 3 biological replicates. Data are expressed as mean ± SD. *p <0.05, one-way ANOVA with the *post hoc* Scheffé test. AP-1, activator protein 1; ChIP, chromatin immunoprecipitation; CREB, cAMP response element binding protein; Egr1, early growth response 1; ETS, E26 transformation-specific; GFP, green fluorescent protein; PA, palmitate; qPCR, quantitative PCR; SCR, scrambled siRNAs; siRNA, small interfering RNA; SRF, serum response factor.

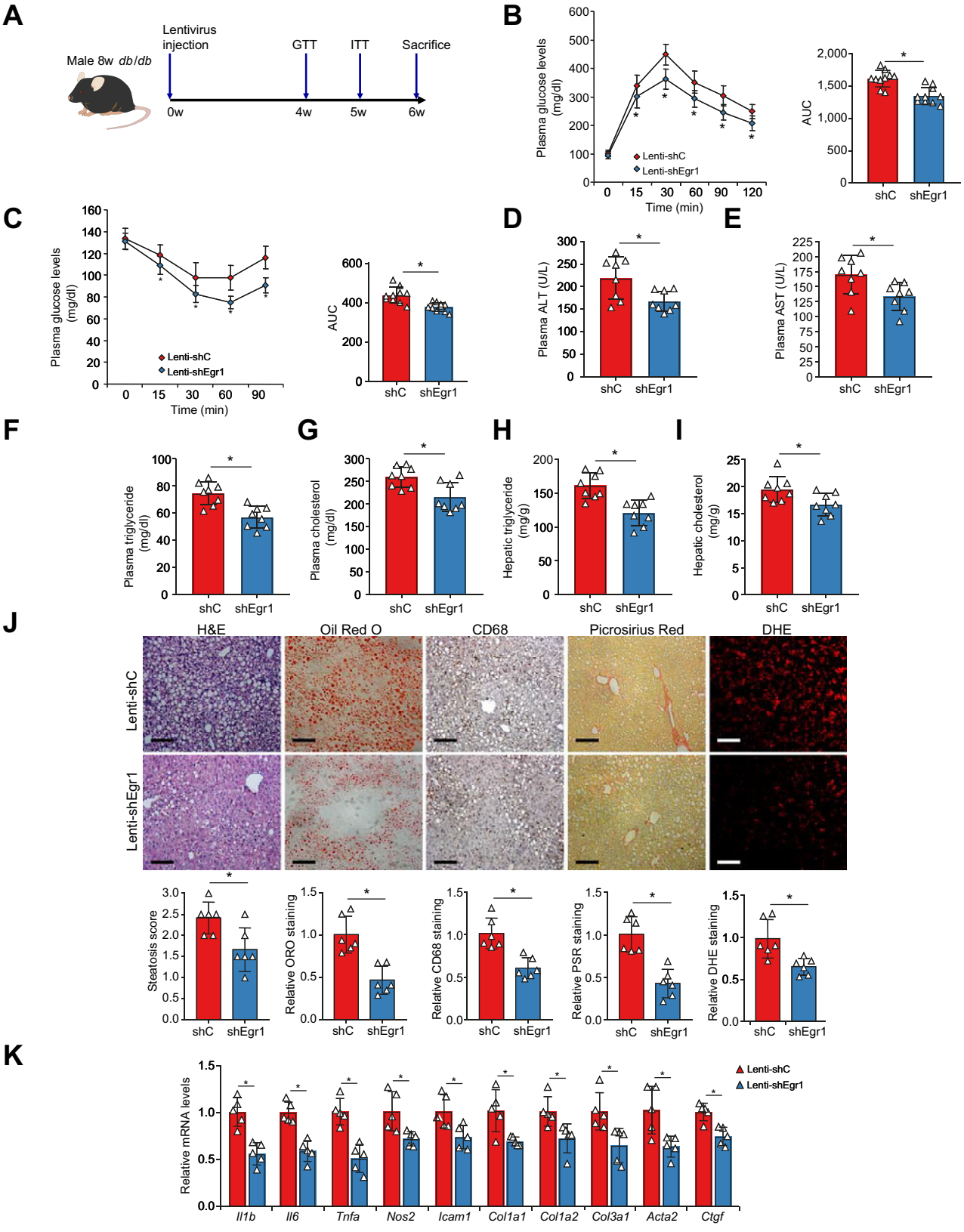

Fig. 3. Egr1 depletion attenuates NAFLD in mice. Lenti-shEgr1 or Lenti-shC was injected into *db*/*db* mice as described in the Materials and methods section. (A) Scheme of protocol. (B) GTT. (C) ITT. (D) Plasma ALT levels. (E) Plasma AST levels. (F) Plasma triglyceride levels. (G) Plasma total cholesterol levels. (H) Hepatic triglyceride levels. (I) Hepatic total cholesterol levels. (J) Paraffin sections were stained with H&E, ORO, PSR, and anti-CD68. (K) Pro-inflammatory and pro-fibrogenic genes were examined by qPCR. N = 5–10 mice for each group. Data are expressed as mean ± SD. $^{*}p$ <0.05, two-tailed Student's *t* test. ALT, alanine transaminase; AST, aspartate aminotransferase; DHE, dihydroethidium; Egr1, early growth response 1; GTT, glucose tolerance test; ITT, insulin tolerance test; Lenti-shC, lentivirus carrying a control shRNA; Lenti-shEgr1, lentivirus carrying shRNA targeting Egr1; ORO, Oil Red O; PSR, Picrosirius Red; qPCR, quantitative PCR; shC, control shRNA; shEgr1, shRNA targeting Egr1; shRNA, small-hairpin RNA.

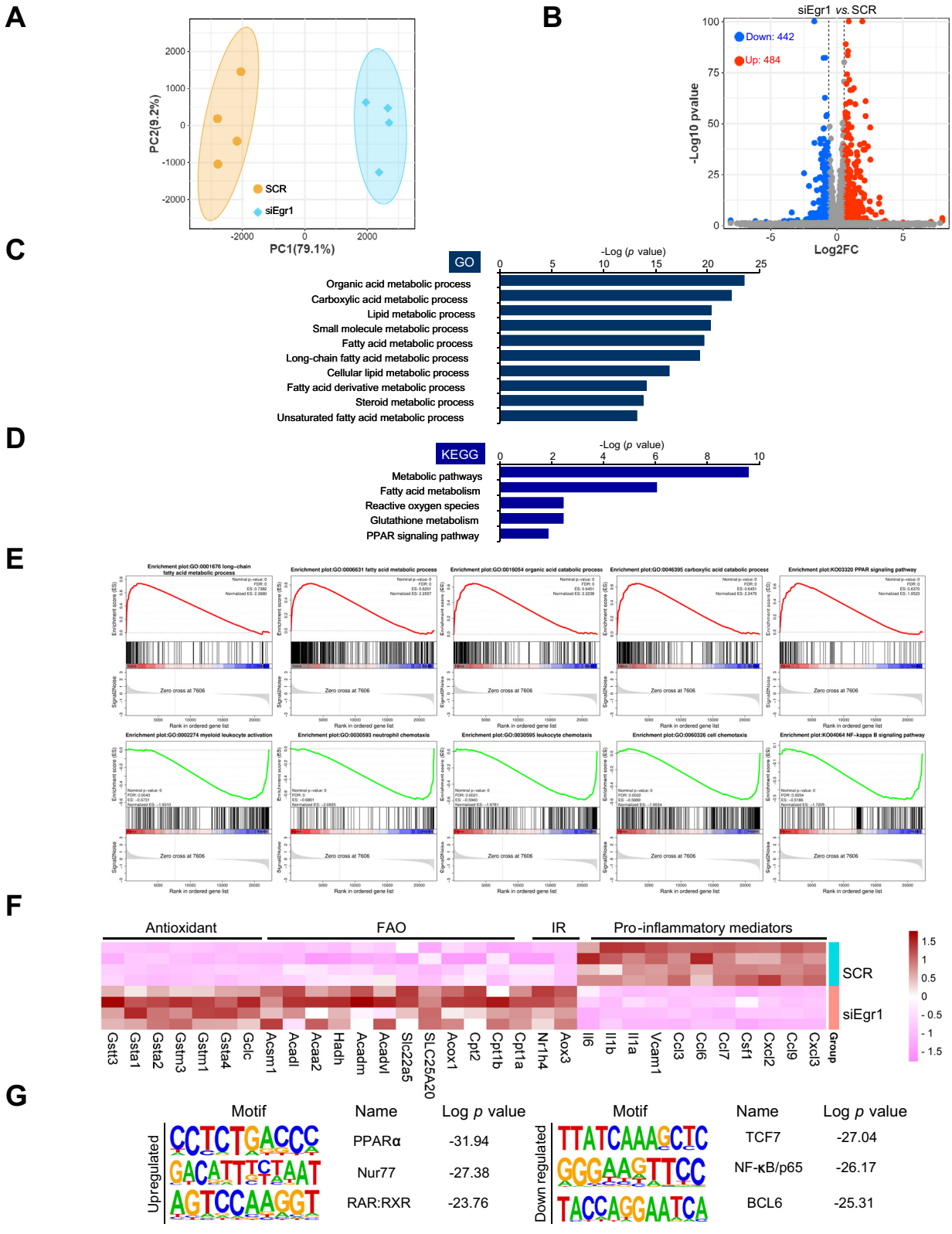

Fig. 4. Egr1 knockdown alters transcriptome in hepatocytes. (A–G) Primary murine hepatocytes were transfected with indicated siRNAs followed by treatment with PA (0.2 mM). RNA-seq was performed and analysed as described in the Materials and methods section. (A) PCA plot. (B) Volcano plot. (C) GO analysis. (D) KEGG analysis. (E) GSEA. (F) Heatmap of differentially expressed genes. (G) HOMER analysis. BCL6, B-cell lymphoma 6; Egr1, early growth response 1; ES, enrichment score; FAO, fatty acid oxidation; FDR, false discovery rate; GO, gene ontology; GSEA, gene set enrichment analysis; HOMER, hypergeometric optimisation of motif enrichment; IR, insulin resistance; KEGG, Kyoto Encyclopedia of Genes and Genomes; PA, palmitate; PC1, principal component 1; PC2, principal component 2; PCA, principal component analysis; PPARα, peroxisome proliferator-activated receptor α; RAR: retinoic acid receptor; RNA-seq, RNA sequencing; RXR, retinoic X receptor; SCR, scrambled siRNAs; siEgr1, Egr1 siRNA; siRNA, small interfering RNA; TCF7, transcription factor 7.

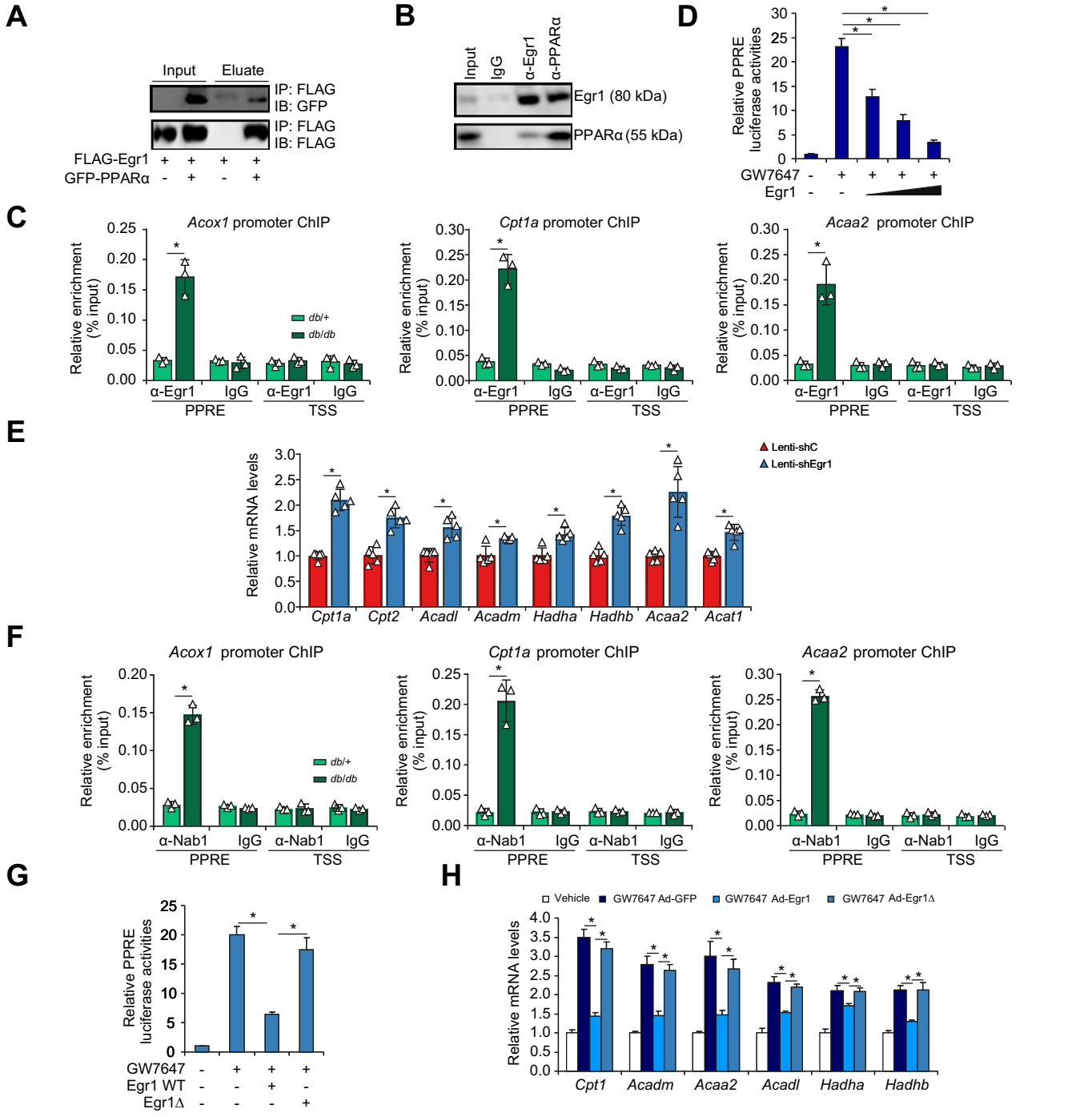

Fig. 5. Erg1 interacts with PPARα to repress FAO transcription. (A) FLAG-tagged Egr1 and GFP-tagged PPARα were transfected into HEK293 cells. Immunoprecipitation was performed with indicated antibodies. (B) Liver lysates from *db*/*db* mice were immunoprecipitated with indicated antibodies. (C) ChIP assay was performed with anti-Egr1 or IgG using liver lysates from *db*/*db* mice and *db*/+ mice. N = 3 mice for each group. Data are expressed as mean ± SD. **p* <0.05, one-way ANOVA with the *post hoc* Scheffé test. (D) A PPRE reporter was transfected into HepaRG cells with increasing doses of Egr1 followed by treatment with GW7647 (0.1 μM). Luciferase activities were normalised by protein concentration and GFP fluorescence. N = 3 biological replicates. Data are expressed as mean ± SD. **p* <0.05, one-way ANOVA with the *post hoc* Scheffé test. (E) Lenti-shEgr1 or Lenti-shC was injected into *db*/*db* mice. Gene expression levels were examined by qPCR. N = 5 mice for each group. Data are expressed as mean ± SD. **p* <0.05, two-tailed Student's *t* test. (F) ChIP assay was performed with anti-Nab1 or IgG using liver lysates from *db*/*db* mice and *db*/+ mice. N = 3 mice for each group. Data are expressed as mean ± SD. **p* <0.05, one-way ANOVA with the *post hoc* Scheffé test. (G) A PPRE reporter was transfected into HepaRG cells with indicated Egr1 vectors followed by treatment with GW7647 (0.1 μM). Luciferase activities were normalised by protein concentration and GFP fluorescence. N = 3 biological replicates. Data are expressed as mean ± SD. **p* <0.05, one-way ANOVA with the *post hoc* Scheffé test. (H) HepaRG cells were transduced with Ad-Egr1, Ad-Egr1Δ, or Ad-GFP followed by treatment with GW7647 (0.1 μM). FAO genes were examined by qPCR. N = 3 biological replicates. Data are expressed as mean ± SD. **p* <0.05, one-way ANOVA with the *post hoc* Scheffé test. Ad-Egr1, adenovirus carrying Egr1; Ad-Egr1Δ, adenovirus carrying Egr1 mutant; Ad-GFP, adenovirus carrying a control vector; ChIP, chromatin immunoprecipitation; Erg1, early growth response 1; FAO, fatty acid oxidation; GFP, green fluorescent protein; IB, immunoblotting; IP, immunoprecipitation; Lenti-shC, lentivirus carrying a control shRNA; Lenti-shEgr1, lentivirus carrying shRNA targeting Egr1; Nab1, NGFI-A binding protein 1; PPARα, peroxisome proliferator-activated receptor α; PPRE, PPAR response element; qPCR, quantitative PCR; shRNA, small-hairpin RNA; TSS, transcription start site; WT, wild-type.

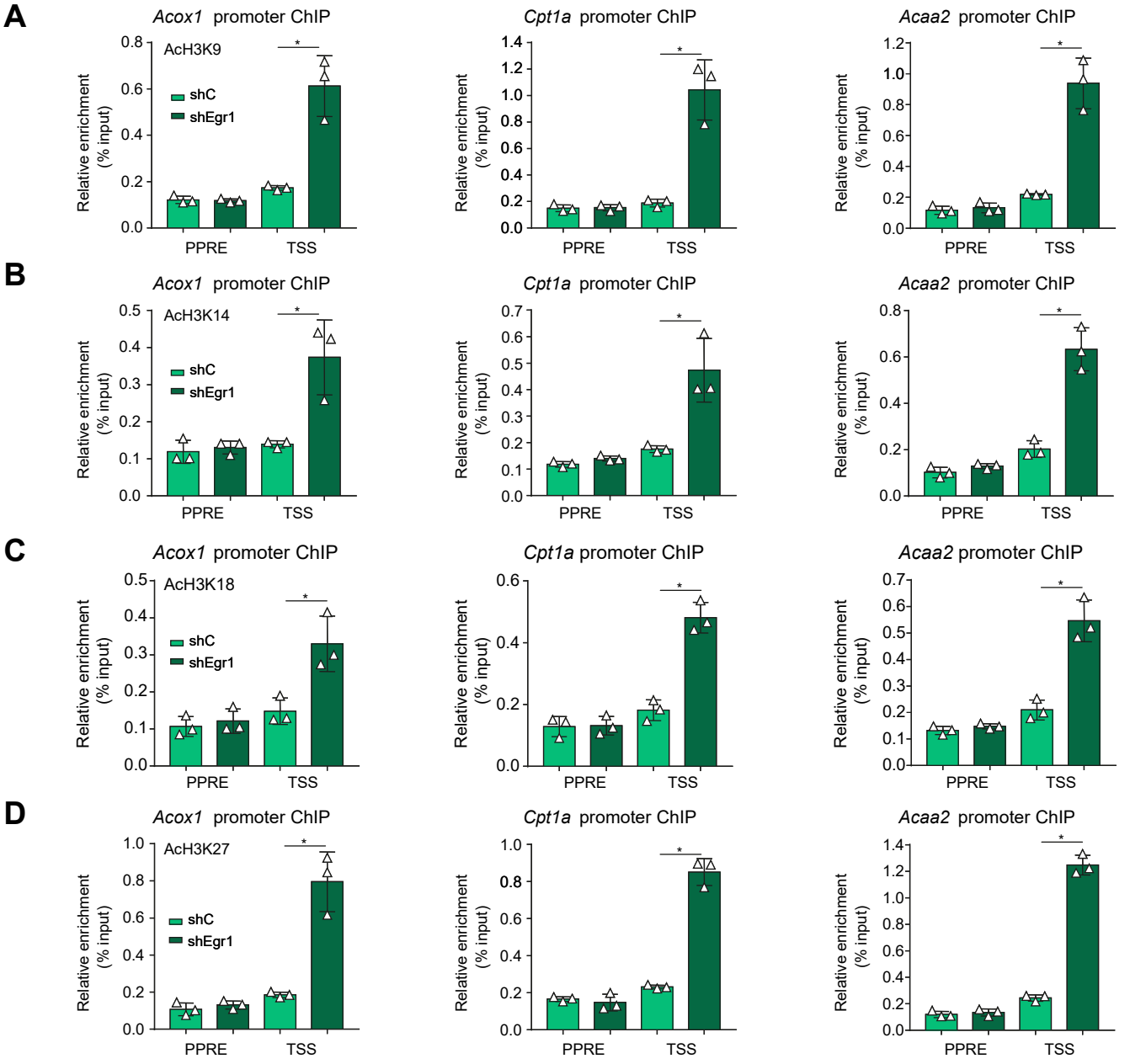

Fig. 6. Erg1 regulates FAO transcription by promoting histone deacetylation. (A–D) Lenti-shEgr1 or Lenti-shC was injected into *db*/*db* mice. ChIP assays were performed with anti-acetyl H3K9 (A), anti-acetyl H3K14 (B), anti-acetyl H3K18 (C), and anti-acetyl H3K27 (D). N = 3 mice for each group. Data are expressed as mean ± SD. **p* <0.05, one-way ANOVA with the *post hoc* Scheffé test. ChIP, chromatin immunoprecipitation; Erg1, early growth response 1; FAO, fatty acid oxidation; Lenti-shC, lentivirus carrying a control shRNA; Lenti-shEgr1, lentivirus carrying shRNA targeting Egr1; PPAR, peroxisome proliferator-activated receptor; PPRE, PPAR response element; shC, control shRNA; shEgr1, shRNA targeting Egr1; shRNA, small-hairpin RNA.

Egr1 expression can be upregulated by a long list of oxygen-free radicals in vascular smooth muscle cells,[55] osteoblasts,[56] myelocytic cells,[57] and tubular epithelial cells.[58] The precise mechanism whereby Egr1 regulates cell-specific redox status is not entirely clear. Recently, Pang *et al.*[59] have made an interesting observation that Egr1 suppresses macrophage phagocytosis by reducing the expression of P62, thus depriving Nrf2, the master regulator of anti-oxidative transcription, a key co-factor.[59] Because increased ROS production and/or impaired ROS clearance is a hallmark event in NAFLD pathogenesis,[60] targeting Egr1 could certainly help restore redox homoeostasis in the liver.

Despite the advances proffered by our study, major limitations exist that dampen enthusiasm. First, lentiviral delivery of shRNA, although driven by a hepatocyte-specific (TBG) promoter, may non-specifically target cell lineages other than hepatocytes. Thus, the observed phenotype could be accounted for by Egr1 in macrophages or sinusoidal endothelial cells. New mouse strains with lineage-specific manipulation of Egr1 expression would help clarify this issue. Second, the regulatory role of Egr1 in

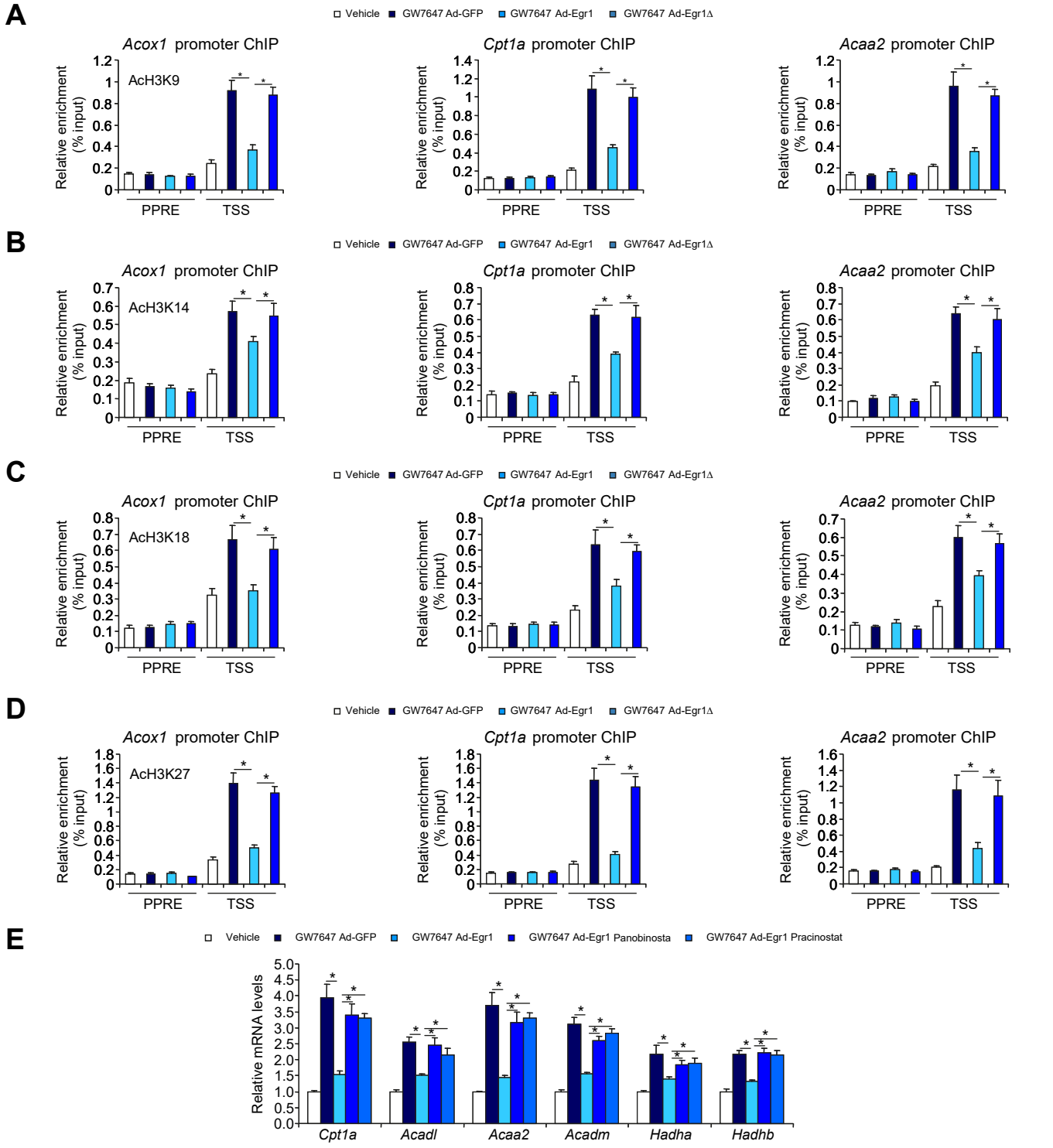

Fig. 7. Erg1 regulates FAO transcription via Nab1-dependent recruitment of HDACs. (A–D) HepaRG cell were transduced with Ad-Egr1, Ad-Egr1Δ, or Ad-GFP followed by treatment with GW7647 (0.1 μM). ChIP assays were performed with anti-acetyl H3K9 (A), anti-acetyl H3K14 (B), anti-acetyl H3K18 (C), and anti-acetyl H3K27 (D). N = 3 biological replicates. Data are expressed as mean ± SD. *p <0.05, one-way ANOVA with the *post hoc* Scheffé test. (E) HepaRG cell were transduced with Ad-Egr1 or Ad-GFP followed by treatment with GW7647 (0.1 μM) in the presence or absence of two pan-HDAC inhibitors (panobinostat [0.1 μM] and pracinostat [0.5 μM]). FAO genes were examined by qPCR. N = 3 biological replicates. Data are expressed as mean ± SD. *p <0.05, one-way ANOVA with the *post hoc* Scheffé test. Ad-Egr1, adenovirus carrying Egr1; Ad-Egr1Δ, adenovirus carrying Egr1 mutant; Ad-GFP, adenovirus carrying a control vector; ChIP, chromatin immunoprecipitation; Erg1, early growth response 1; FAO, fatty acid oxidation; GFP, green fluorescent protein; HDAC, histone deacetylase; Nab1, NGFI-A binding protein 1; PPAR, peroxisome proliferator-activated receptor; PPRE, PPAR response element; qPCR, quantitative PCR.

NAFLD pathogenesis was investigated in a single mouse model, the genetically predisposed *db*/*db* model, considered not ideal in terms of recapitulating the human NAFLD-NASH pathology owing to low level of liver fibrosis and low incidence of hepatocellular carcinoma.[61] Future studies should exploit multiple and preferably humanised NAFLD-NASH models to validate the regulatory role of Egr1.

In summary, our data provide novel mechanistic insight on Egr1 upregulation during NAFLD pathogenesis. More importantly, our data suggest that Egr1 regulates a transcriptional programme in hepatocytes that might contribute to NAFLD. Further studies should be conducted to provide genetic evidence that links Egr1 to NAFLD in experimental animals and in humans to justify targeting Egr1 for NAFLD intervention.

Abbreviations

Ad-Egr1, adenovirus carrying Egr1; Ad-Egr1Δ, adenovirus carrying Egr1 mutant; Ad-GFP, adenovirus carrying a control vector; ALT, alanine transaminase; AP-1, activator protein 1; AST, aspartate aminotransferase; CD, control diet; CDA-HFD, choline-deficient, L-amino acid-defined HFD; ChIP, chromatin immunoprecipitation; ChREBP, carbohydrate response element binding protein; CREB, cAMP response element binding protein; DEG, differentially expressed gene; DHE, dihydroethidium; Egr1, early growth response 1; ETS, E26 transformation-specific; FAO, fatty acid oxidation; FFA, free fatty acids; FGF21, fibroblast growth factor 21; FPKM, fragments per kilobase of exon model per million reads mapped; GFP, green fluorescent protein; GO, gene ontology; GSEA, gene set enrichment analysis; GTT, glucose tolerance test; HDAC, histone deacetylase; HDACi, HDAC inhibitor; HFD, high-fat diet; HOMER, hypergeometric optimisation of motif enrichment; HRP, horseradish peroxidase; ITT, insulin tolerance test; KEGG, Kyoto Encyclopedia of Genes and Genomes; Lenti-shC, lentivirus carrying a control shRNA; Lenti-shEgr1, lentivirus carrying shRNA targeting Egr1; MCP1, monocyte chemoattractant protein 1; Nab-1, NGFI-A binding protein 1; NAFLD, non-alcoholic fatty liver disease; NASH, non-alcoholic steatohepatitis; ORO, Oil Red O; PA, palmitate; PPARα, peroxisome proliferator-activated receptor α; PPRE, PPAR response element; PSR, Picrosirius Red; qPCR, quantitative PCR; RNA-seq, RNA sequencing; ROS, reactive oxygen species; SCR, scrambled siRNAs; shC, control shRNA; shEgr1, shRNA targeting Egr1; shRNA, small-hairpin RNA; siRNA, small interfering RNA; SRF, serum response factor; TBG, thyroxin-binding globulin; TG, triglyceride; TRAF3, Tumour necrosis factor receptor-associated factor 3; WT, wild-type.

Financial support

This work was supported by grants from the National Natural Science Foundation of China (82170592, 82200684, and 81900513), the Natural Science Foundation of Jiangsu Province (BK20221032), and Liaocheng University (318012118).

Conflicts of interest

The authors delare no conflict of interest.

Please refer to the accompanying ICMJE disclosure forms for further details.

Authors' contributions

Conceived the project: ZWF, ZLL, QHW. Designed experiments: all authors. Performed experiments, collected data, and analysed data: YG, XLM, XYS, LYL, AQZ, XZ, ZLL, ZWF. Secured funding: ZLL, ZWF. Drafted the manuscript: YX. Edited and finalised the manuscript: all authors.

Data availability statement

The data that support the findings of this study are available upon reasonable request.

Supplementary data

Supplementary data to this article can be found online at https://doi.org/10.1016/j.jhepr.2023.100724.

References

[1] Cotter TG, Rinella M. Nonalcoholic fatty liver disease 2020: the state of the disease. Gastroenterology 2020;158:1851–1864.
[2] Anstee QM, Reeves HL, Kotsiliti E, Govaere O, Heikenwalder M. From NASH to HCC: current concepts and future challenges. Nat Rev Gastroenterol Hepatol 2019;16:411–428.
[3] Godoy-Matos AF, Silva Júnior WS, Valerio CM. NAFLD as a continuum: from obesity to metabolic syndrome and diabetes. Diabetol Metab Syndr 2020;12:60.
[4] Abdelmalek MF. Nonalcoholic fatty liver disease: another leap forward. Nat Rev Gastroenterol Hepatol 2021;18:85–86.
[5] Zhu L, Baker SS, Liu W, Tao MH, Patel R, Nowak NJ, et al. Lipid in the livers of adolescents with nonalcoholic steatohepatitis: combined effects of pathways on steatosis. Metabolism 2011;60:1001–1011.
[6] Dorn C, Riener MO, Kirovski G, Saugspier M, Steib K, Weiss TS, et al. Expression of fatty acid synthase in nonalcoholic fatty liver disease. Int J Clin Exp Pathol 2010;3:505–514.
[7] Xie Z, Li H, Wang K, Lin J, Wang Q, Zhao G, et al. Analysis of transcriptome and metabolome profiles alterations in fatty liver induced by high-fat diet in rat. Metabolism 2010;59:554–560.
[8] Croci I, Byrne NM, Choquette S, Hills AP, Chachay VS, Clouston AD, et al. Whole-body substrate metabolism is associated with disease severity in patients with non-alcoholic fatty liver disease. Gut 2013;62:1625–1633.
[9] Fujita K, Nozaki Y, Wada K, Yoneda M, Fujimoto Y, Fujitake M, et al. Dysfunctional very-low-density lipoprotein synthesis and release is a key factor in nonalcoholic steatohepatitis pathogenesis. Hepatology 2009;50:772–780.
[10] Wang PX, Zhang XJ, Luo P, Jiang X, Zhang P, Guo J, et al. Hepatocyte TRAF3 promotes liver steatosis and systemic insulin resistance through targeting TAK1-dependent signalling. Nat Commun 2016;7:10592.
[11] Van Beek M, Oravecz-Wilson KI, Delekta PC, Gu S, Li X, Jin X, et al. Bcl10 links saturated fat overnutrition with hepatocellular NF-κB activation and insulin resistance. Cell Rep 2012;1:444–452.
[12] Reboldi A, Dang EV, McDonald JG, Liang G, Russell DW, Cyster JG. Inflammation. 25-Hydroxycholesterol suppresses interleukin-1-driven inflammation downstream of type I interferon. Science 2014;345:679–684.
[13] Im SS, Yousef L, Blaschitz C, Liu JZ, Edwards RA, Young SG, et al. Linking lipid metabolism to the innate immune response in macrophages through sterol regulatory element binding protein-1a. Cell Metab 2011;13:540–549.
[14] Oishi Y, Spann NJ, Link VM, Muse ED, Strid T, Edillor C, et al. SREBP1 contributes to resolution of pro-inflammatory TLR4 signaling by reprogramming fatty acid metabolism. Cel Metab 2017;25:412–427.
[15] Daniel PV, Dogra S, Rawat P, Choubey A, Khan AS, Rajak S, et al. NF-κB p65 regulates hepatic lipogenesis by promoting nuclear entry of ChREBP in response to a high carbohydrate diet. J Biol Chem 2021;296:100714.
[16] Pérez-Schindler J, Vargas-Fernández E, Karrer-Cardel B, Ritz D, Schmidt A, Handschin C. Characterization of regulatory transcriptional mechanisms in hepatocyte lipotoxicity. Sci Rep 2022;12:11477.
[17] Wright JJ, Gunter KC, Mitsuya H, Irving SG, Kelly K, Siebenlist U. Expression of a zinc finger gene in HTLV-I- and HTLV-II-transformed cells. Science 1990;248:588–591.
[18] Siderovski DP, Blum S, Forsdyke RE, Forsdyke DR. A set of human putative lymphocyte G0/G1 switch genes includes genes homologous to rodent cytokine and zinc finger protein-encoding genes. DNA Cel Biol 1990;9:579–587.
[19] Wang B, Guo H, Yu H, Chen Y, Xu H, Zhao G. The role of the transcription factor EGR1 in cancer. Front Oncol 2021;11:642547.
[20] Banerji R, Saroj SD. Early growth response 1 (EGR1) activation in initial stages of host–pathogen interactions. Mol Biol Rep 2021;48:2935–2943.
[21] Bhattacharyya S, Fang F, Tourtellotte W, Varga J. Egr-1: new conductor for the tissue repair orchestra directs harmony (regeneration) or cacophony (fibrosis). J Pathol 2013;229:286–297.

[22] McMullen MR, Pritchard MT, Wang Q, Millward CA, Croniger CM, Nagy LE. Early growth response-1 transcription factor is essential for ethanol-induced fatty liver injury in mice. Gastroenterology 2005;128:2066–2076.
[23] Matsumoto M, Hada N, Sakamaki Y, Uno A, Shiga T, Tanaka C, et al. An improved mouse model that rapidly develops fibrosis in non-alcoholic steatohepatitis. Int J Exp Pathol 2013;94:93–103.
[24] Dong W, Zhu Y, Zhang Y, Fan Z, Zhang Z, Fan X, et al. BRG1 links TLR4 trans-activation to LPS-induced SREBP1a expression and liver injury. Front Cel Dev Biol 2021;9:617073.
[25] Fan Z, Kong M, Miao X, Guo Y, Ren H, Wang J, et al. An E2F5-TFDP1-BRG1 complex mediates transcriptional activation of MYCN in hepatocytes. Front Cel Dev Biol 2021;9:742319.
[26] Lv F, Shao T, Xue Y, Miao X, Guo Y, Wang Y, et al. Dual regulation of tank binding kinase 1 (TBK1) by BRG1 in hepatocytes contributes to ROS production. Front Cel Dev Biol 2021;9:745985.
[27] Kong M, Dong W, Zhu Y, Fan Z, Miao X, Guo Y, et al. Redox-sensitive activation of CCL7 by BRG1 in hepatocytes during liver injury. Redox Biol 2021;46:102079.
[28] Kong M, Dong W, Xu H, Fan Z, Miao X, Guo Y, et al. Choline kinase alpha is a novel transcriptional target of the Brg1 in hepatocyte: implication in liver regeneration. Front Cel Dev Biol 2021;9:705302.
[29] Chen B, Dong W, Shao T, Miao X, Guo Y, Liu X, et al. A KDM4-DBC1-SIRT1 axis contributes to TGF-b induced mesenchymal transition of intestinal epithelial cells. Front Cel Dev Biol 2021;9:697614.
[30] Chen B, Zhu Y, Chen J, Feng Y, Xu Y. Activation of TC10-like transcription by lysine demethylase KDM4B in colorectal cancer cells. Front Cel Dev Biol 2021;9:617549.
[31] Fan Z, Kong M, Dong W, Dong C, Miao X, Guo Y, et al. Trans-activation of eotaxin-1 by Brg1 contributes to liver regeneration. Cell Death Dis 2022;13:495.
[32] Dong W, Kong M, Liu H, Xue Y, Li Z, Wang Y, et al. Myocardin-related transcription factor A drives ROS-fueled expansion of hepatic stellate cells by regulating p38-MAPK signalling. Clin Transl Med 2022;12:e688.
[33] Wu X, Dong W, Kong M, Ren H, Wang J, Shang L, et al. Down-regulation of CXXC5 de-represses MYCL1 to promote hepatic stellate cell activation. Front Cel Dev Biol 2021;9:680344.
[34] Feldstein AE, Werneburg NW, Canbay A, Guicciardi ME, Bronk SF, Rydzewski R, et al. Free fatty acids promote hepatic lipotoxicity by stimulating TNF-α expression via a lysosomal pathway. Hepatology 2004;40:185–194.
[35] Jensen T, Abdelmalek MF, Sullivan S, Nadeau KJ, Green M, Roncal C, et al. Fructose and sugar: a major mediator of non-alcoholic fatty liver disease. J Hepatol 2018;68:1063–1075.
[36] Inagaki T, Dutchak P, Zhao G, Ding X, Gautron L, Parameswara V, et al. Endocrine regulation of the fasting response by PPARα-mediated induction of fibroblast growth factor 21. Cel Metab 2007;5:415–425.
[37] Badman MK, Pissios P, Kennedy AR, Koukos G, Flier JS, Maratos-Flier E. Hepatic fibroblast growth factor 21 is regulated by PPARα and is a key mediator of hepatic lipid metabolism in ketotic states. Cel Metab 2007;5:426–437.
[38] Russo MW, Sevetson BR, Milbrandt J. Identification of NAB1, a repressor of NGFI-A- and Krox20-mediated transcription. Proc Natl Acad Sci USA 1995;92:6873–6877.
[39] Liu C, Adamson E, Mercola D. Transcription factor EGR-1 suppresses the growth and transformation of human HT-1080 fibrosarcoma cells by induction of transforming growth factor beta 1. Proc Natl Acad Sci USA 1996;93:11831–11836.
[40] Parthasarathy G, Revelo X, Malhi H. Pathogenesis of nonalcoholic steatohepatitis: an overview. Hepatol Commun 2020;4:478–492.
[41] Kang B, Kang B, Roh TY, Seong RH, Kim W. The chromatin accessibility landscape of nonalcoholic fatty liver disease progression. Mol Cell 2022;45:343–352.
[42] Lin C, Hindes A, Burns CJ, Koppel AC, Kiss A, Yin Y, et al. Serum response factor controls transcriptional network regulating epidermal function and hair follicle morphogenesis. J Invest Dermatol 2013;133:608–617.
[43] Kong M, Chen X, Lv F, Ren H, Fan Z, Qin H, et al. Serum response factor (SRF) promotes ROS generation and hepatic stellate cell activation by epigenetically stimulating NCF1/2 transcription. Redox Biol 2019;26:101302.
[44] Rosenwald M, Efthymiou V, Opitz L, Wolfrum C. SRF and MKL1 independently inhibit Brown adipogenesis. PLoS One 2017;12:e0170643.
[45] Sun K, Battle MA, Misra RP, Duncan SA. Hepatocyte expression of serum response factor is essential for liver function, hepatocyte proliferation and survival, and postnatal body growth in mice. Hepatology 2009;49:1645–1654.
[46] Jin W, Goldfine AB, Boes T, Henry RR, Ciaraldi TP, Kim EY, et al. Increased SRF transcriptional activity in human and mouse skeletal muscle is a signature of insulin resistance. J Clin Invest 2011;121:918–929.
[47] Sun Z, Feng D, Fang B, Mullican SE, You SH, Lim HW, et al. Deacetylase-independent function of HDAC3 in transcription and metabolism requires nuclear receptor corepressor. Mol Cel 2013;52:769–782.
[48] Qiu X, Li J, Lv S, Yu J, Jiang J, Yao J, et al. HDAC5 integrates ER stress and fasting signals to regulate hepatic fatty acid oxidation. J Lipid Res 2018;59:330–338.
[50] Donde H, Ghare S, Joshi-Barve S, Zhang J, Vadhanam MV, Gobejishvili L, et al. Tributyrin inhibits ethanol-induced epigenetic repression of CPT-1A and attenuates hepatic steatosis and injury. Cell Mol Gastroenterol Hepatol 2020;9:569–585.
[51] Pawlinski R, Pedersen B, Kehrle B, Aird WC, Frank RD, Guha M, et al. Regulation of tissue factor and inflammatory mediators by Egr-1 in a mouse endotoxemia model. Blood 2003;101:3940–3947.
[52] Cho SJ, Kang MJ, Homer RJ, Kang HR, Zhang X, Lee PJ, et al. Role of early growth response-1 (Egr-1) in interleukin-13-induced inflammation and remodeling. J Biol Chem 2006;281:8161–8168.
[53] Albrecht C, Preusch MR, Hofmann G, Morris-Rosenfeld S, Blessing E, Rosenfeld ME, et al. Egr-1 deficiency in bone marrow-derived cells reduces atherosclerotic lesion formation in a hyperlipidaemic mouse model. Cardiovasc Res 2010;86:321–329.
[54] Trizzino M, Zucco A, Deliard S, Wang F, Barbieri E, Veglia F, et al. EGR1 is a gatekeeper of inflammatory enhancers in human macrophages. Sci Adv 2021;7:eaaz8836.
[55] Hasan RN, Schafer AI. Hemin upregulates Egr-1 expression in vascular smooth muscle cells via reactive oxygen species ERK-1/2-Elk-1 and NF-κB. Circ Res 2008;102:42–50.
[56] Nose K, Ohba M. Functional activation of the egr-1 (early growth response-1) gene by hydrogen peroxide. Biochem J 1996;316:381κ3.
[57] Datta R, Taneja N, Sukhatme VP, Qureshi SA, Weichselbaum R, Kufe DW. Reactive oxygen intermediates target CC(A/T)6GG sequences to mediate activation of the early growth response 1 transcription factor gene by ionizing radiation. Proc Natl Acad Sci USA 1993;90:2419–2422.
[58] Bek MJ, Reinhardt HC, Fischer KG, Hirsch JR, Hupfer C, Dayal E, et al. Up-regulation of early growth response gene-1 via the CXCR3 receptor induces reactive oxygen species and inhibits Na^+/K^+-ATPase activity in an immortalized human proximal tubule cell line. J Immunol 2003;170:931–940.
[59] Pang Z, Xu Y, Zhu Q. Early growth response 1 suppresses macrophage phagocytosis by inhibiting NRF2 activation through upregulation of autophagy during *Pseudomonas aeruginosa* infection. Front Cel Infect Microbiol 2021;11:773665.
[60] Chen Z, Tian R, She Z, Cai J, Li H. Role of oxidative stress in the pathogenesis of nonalcoholic fatty liver disease. Free Radic Biol Med 2020;152:116–141.
[61] Farrell G, Schattenberg JM, Leclercq I, Yeh MM, Goldin R, Teoh N, et al. Mouse models of nonalcoholic steatohepatitis: toward optimization of their relevance to human nonalcoholic steatohepatitis. Hepatology 2019;69:2241–2257.

Journal of Hepatology, Volume *5*

Supplemental information

Zinc finger transcription factor Egf1 promotes non-alcoholic fatty liver disease

Yan Guo, Xiulian Miao, Xinyue Sun, Luyang Li, Anqi Zhou, Xi Zhu, Yong Xu, Qinghua Wang, Zilong Li, and Zhiwen Fan

Zinc finger transcription factor Egf1 promotes non-alcoholic fatty liver disease

Yan Guo, Xiulian Miao, Xinyue Sun, Luyang Li, Anqi Zhou, Xi Zhu, Yong Xu, Qinghua Wang, Zilong Li, Zhiwen Fan

Table of contents

Fig. S1……Page 2
Fig. S2……Page 3
Fig. S3……Page 4
Fig. S4……Page 5
Fig. S5……Page 6
Fig. S6……Page 7
Fig. S7……Page 8
Fig. S8……Page 9
Fig. S9……Page 10
Fig. S10……Page 11
Fig. S11……Page 12
Fig. S12……Page 13
Fig. S13……Page 14
Fig. S14……Page 15
Fig. S15……Page 16

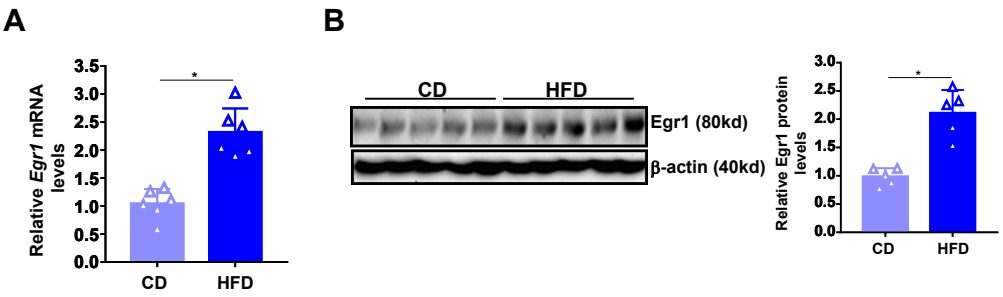

Fig. S1: (**A, B**) C57/B6 mice were fed on a high-fat diet (HFD) or a control diet (CD) for 12 weeks. Egr1 expression was examined by qPCR and western blotting. N=6 mice for each group.

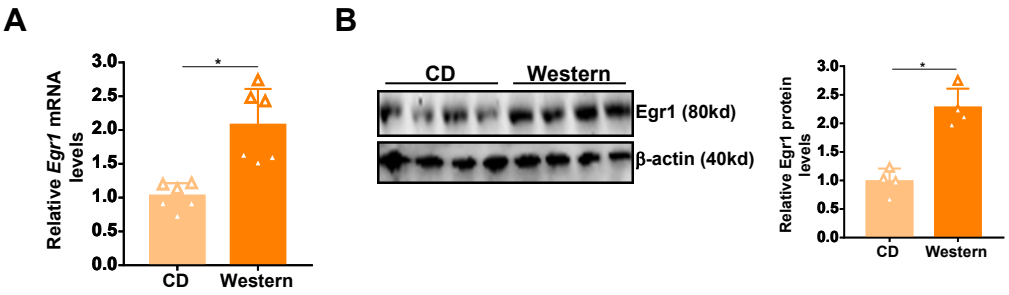

Fig. S2: (**A, B**) *Apoe*$^{-/-}$ mice were fed on a Western diet or a control diet (CD) for 7 weeks. Egr1 expression was examined by qPCR and western blotting. N=6 mice for each group.

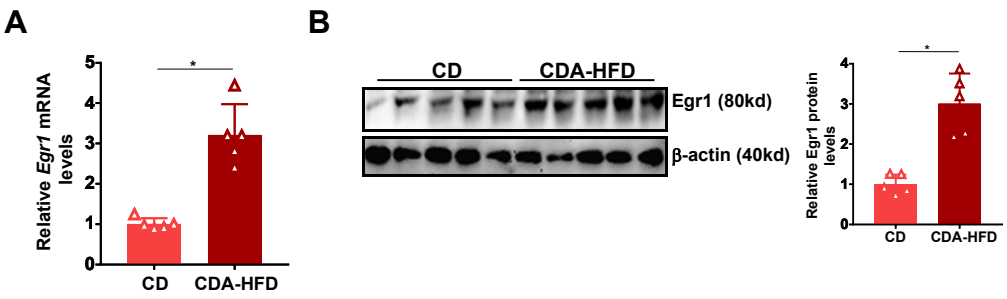

Fig. S3: (**A, B**) C57/B6 mice were fed on CDA-HFD or a control diet (CD) for 8 weeks. Egr1 expression was examined by qPCR and western blotting. N=6 mice for each group.

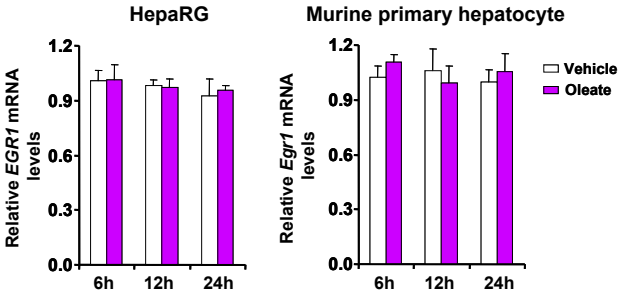

Fig. S4: HepaRG cells and primary murine hepatocytes were treated with or without oleate (0.2mM). EGR1 expression was examined by qPCR.

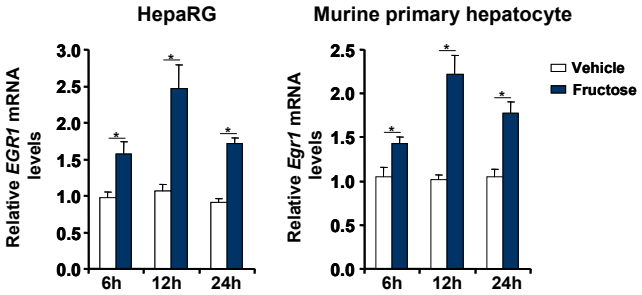

Fig. S5: HepaRG cells and primary murine hepatocytes were treated with or without fructose (10mM). EGR1 expression was examined by qPCR.

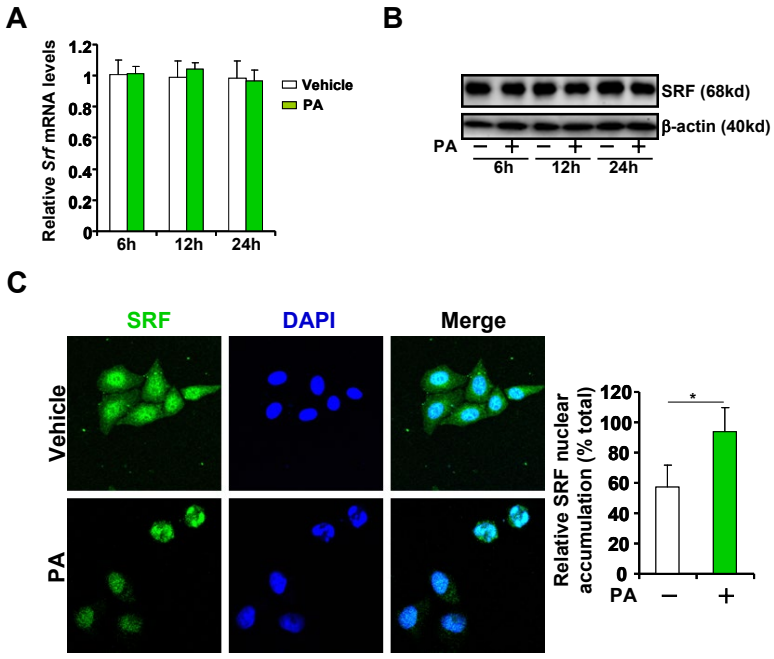

Fig. S6: (**A-C**) Primary hepatocytes were treated with or without palmitate (PA, 0.2mM). SRF expression was examined by qPCR (A) and western blotting (B). SRF sub-cellular localization was examined by immunofluorescence staining (C).

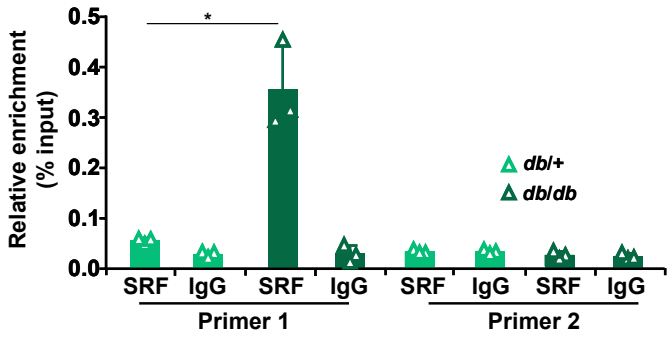

Fig. S7: ChIP assay was performed with anti-SRF or IgG using liver lysates from *db*/*db* mice and *db*/+ mice.

‘

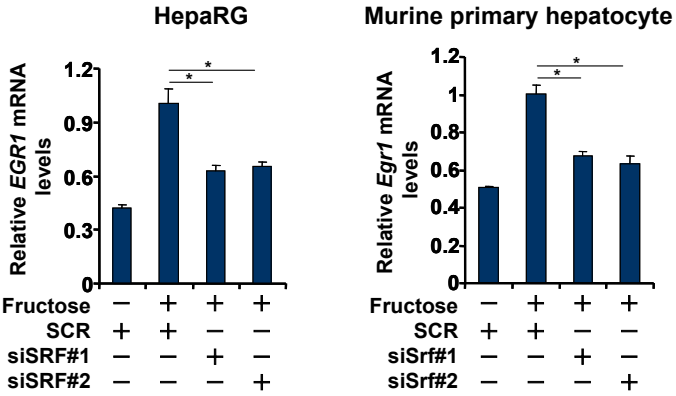

Fig. S8: HepaRG cells and primary murine hepatocytes were transfected with siRNA targeting SRF or scrambled siRNAs (SCR) followed by treatment with fructose (10mM). Egr1 expression was examined by qPCR

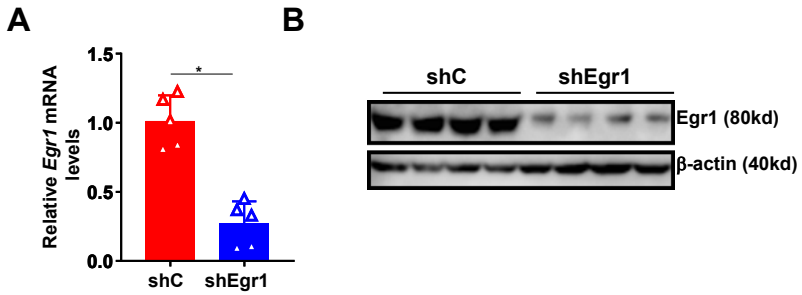

Fig. S9: Lentivirus carrying shRNA targeting Egr1 (Lenti-shEgr1) or a control shRNA (Lenti-shC) was injected into *db*/*db* mice. Egr1 expression was examined by qPCR and western blotting.

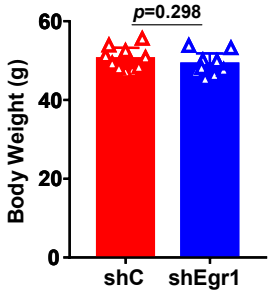

Fig. S10: Lentivirus carrying shRNA targeting Egr1 (Lenti-shEgr1) or a control shRNA (Lenti-shC) was injected into *db*/*db* mice. Egr1 knockdown did not alter body weight of the mice.

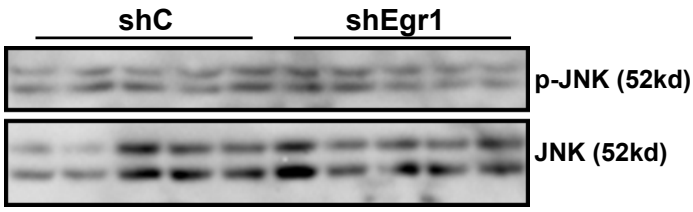

Fig. S11: Lentivirus carrying shRNA targeting Egr1 (Lenti-shEgr1) or a control shRNA (Lenti-shC) was injected into *db*/*db* mice. JNK expression and phosphorylation were examined by western blotting.

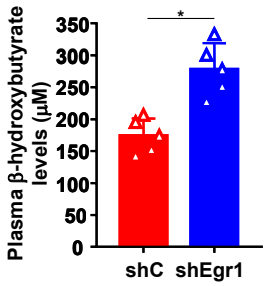

Fig. S12: Lentivirus carrying shRNA targeting Egr1 (Lenti-shEgr1) or a control shRNA (Lenti-shC) was injected into *db*/*db* mice. Plasma □-hydroxybutyrate was measured by a commercially available kit.

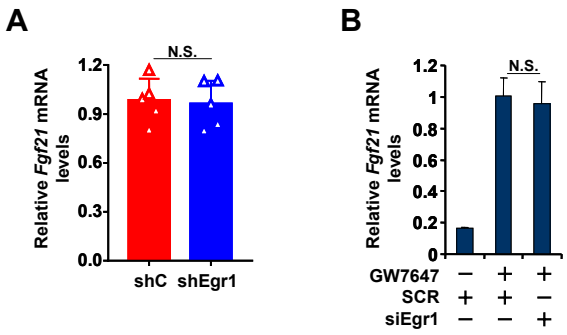

Fig. S13: (**A**) Lentivirus carrying shRNA targeting Egr1 (Lenti-shEgr1) or a control shRNA (Lenti-shC) was injected into *db*/*db* mice. Hepatic FGF21 expression was examined by qPCR. (B) Murine primary hepatocytes were transfected with siRNA targeting Egr1 or scrambled siRNAs (SCR) followed by treatment with GW7647 (0.1□M). FGF21 expression was examined by qPCR.

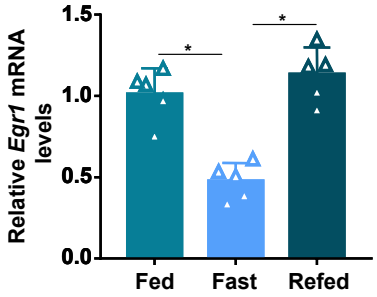

Fig. S14: C57/B6 mice were subjected to 12h of fasting followed by 12h of re-feeding. Hepatic Egr1 expression was examined by qPCR.

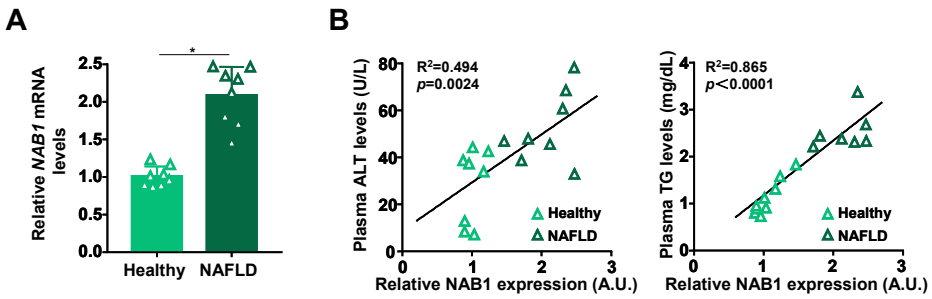

Fig. S15: Nab1 expression levels in the livers of NASH patients and healthy individuals were examined by qPCR. Linear regression was performed by Graphpad Prism. N=8 cases for each group.